

Nariya Cho
Woo Kyung Moon
Jeong-Seon Park

Real-time US elastography in the differentiation of suspicious microcalcifications on mammography

Received: 8 November 2008
Revised: 1 January 2009
Accepted: 10 January 2009
Published online: 18 February 2009
© European Society of Radiology 2009

N. Cho · W. K. Moon
Department of Radiology and Clinical
Research Institute, Seoul National
University Hospital and the Institute of
Radiation Medicine, Seoul National
University Medical Research Center,
Seoul, Republic of Korea

J.-S. Park
Department of Radiology, Hanyang
University College of Medicine,
Hanyang University Hospital,
Seoul, Republic of Korea

W. K. Moon (✉)
Department of Radiology,
Seoul National University Hospital,
28, Yongon-dong, Chongno-gu,
Seoul 100-744, Republic of Korea
e-mail: moonwk@radcom.snu.ac.kr
Tel.: +82-2-7602584
Fax: +82-2-7436385

Abstract The purpose of this study was to retrospectively evaluate the use of US elastography in the differentiation of mammographically detected suspicious microcalcifications, using histology as the reference standard. Between May 2006 and April 2007, real-time US elasticity images were obtained in 77 patients (age range, 24–67 years; mean, 46 years) with 77 mammographically detected areas of microcalcifications (42 benign and 35 malignant lesions) prior to needle biopsy. Two experienced radiologists reviewed cine clips of elasticity and B-mode images and assigned an elasticity score of 1 to 3 in consensus, based on the degree of strain in the hypoechoic lesion without information of mammography and histology. For the elasticity score, the mean \pm standard deviation was 1.5 ± 0.7 for benign and 2.7 ± 0.7 for malignant lesions ($P <$

0.001). When a cutoff point between elasticity scores of 1 and 2 was used, US elastography showed 97% (34/35) sensitivity, 62% (26/42) specificity, 68% (34/50) PPV, and 96% (26/27) NPV with an Az value of 0.852 (0.753–0.923, 95% confidence interval) in the differentiation of benign and malignant microcalcifications. Our results suggest that US elastography has the potential to differentiate benign and malignant lesions associated with microcalcifications detected at screening mammography.

Keywords Breast neoplasms · Calcification · Ultrasound elastography · Tissue characterization

Introduction

Mammography has been accepted as the only modality for the detection and characterization of microcalcifications which are often the only sign of early breast cancer [1]. However, as the specificity of mammography for the differentiation of benign and malignant microcalcifications remains low, ranging from 10–60% [2], approximately 67–78% of percutaneous or surgical biopsies have ultimately proven the microcalcifications to be benign [3–6]. The role of ultrasound (US) for the evaluation of microcalcifications detected at mammography remains controversial, although several studies have shown that microcalcifications can be identified by US in 23–93% of cases and can be sampled by US guidance with a 78–100% success rate [7–9]. The most

common US features of lesions corresponding to both benign and malignant mammographic microcalcifications are ill-defined or microlobulated hypoechoic masses or ductal irregularities [8, 9].

US elastography was developed to depict the relative stiffness of tissue. US echo signals are obtained from a tissue before and after compression, and the amount of displacement relative to the surroundings is converted to an image display [10]. It was reported in a basic study of breast tissue stiffness that fat, normal glandular tissue, fibrous tissue, ductal carcinoma in situ (DCIS), and infiltrating ductal carcinoma (IDC) of the breast had different elastic moduli according to the strain level [11]. Several clinical studies have reported that US elastography had the potential to differentiate between benign and

malignant breast lesions [12–19] and showed similar or inferior diagnostic performance compared with conventional US with a sensitivity of 78.0–86.5% and specificity of 80.9–98.5% [14, 17, 19]. In theory, US elastographic evaluation can be applied for lesions associated with microcalcifications if the lesions are visible at US. However, the literature contains no reports regarding the use of US elastography in the evaluation of microcalcifications on mammography.

The purpose of this study was to retrospectively evaluate the use of US elastography for the differentiation of mammographically detected suspicious microcalcifications, using histology as the reference standard.

Materials and methods

Patients and lesions

Between May 2006 and April 2007, elastographic evaluation of nonpalpable breast lesions was performed for the patients undergoing US-guided percutaneous breast biopsy. Informed consent was obtained from each patient prior to biopsy. The institutional review board approved our study and waived informed consent to perform this retrospective analysis of the cine clips obtained during the prior study.

Eighty-five consecutive women who had been scheduled to undergo US-guided vacuum-assisted biopsy based on suspicious microcalcifications detected at screening mammography were examined using real-time US elastography. Lesions associated with microcalcifications were visualized in previous US images as hypoechoic lesions in all patients and US-guided 11-gauge vacuum-assisted biopsy was performed. Eight women were later excluded due to the absence of calcifications on specimen radiographs ($n=2$), absence of follow-up at least 1 year in women with benign lesions ($n=5$), or no subsequent surgical excision in women with atypical ductal hyperplasia upon needle biopsy ($n=1$). Finally, 77 breast lesions of microcalcifications in 77 women (age range, 24–67 years; mean age, 46 years) were included in this study. A 24-year-old woman underwent screening mammography because her mother and sister were diagnosed with premenopausal breast cancer.

Mammography was performed using a dedicated digital mammography unit (Senographe 2000D FFDM; GE Medical Systems, Milwaukee, WI). Standard mediolateral oblique, craniocaudal mammograms, and additional true lateral, spot compression magnification images of areas containing microcalcifications were obtained from all patients. Mammographic features were retrospectively assessed by a radiologist with 6 years of experience in the interpretation of mammography without information of the histology or elastographic findings. According to the American College of Radiology (ACR) breast imaging

reporting and data system (BI-RADS) [20], three (4%) women had homogeneously fatty breasts (BI-RADS 1 density), 13 (17%) women had scattered fibroglandular tissue (BI-RADS 2 density), 46 (60%) women had heterogeneously dense breasts (BI-RADS 3 density), and 15 (20%) women had extremely dense breasts (BI-RADS 4 density). The mean lesion size of a microcalcification cluster, defined as the greatest diameter on either mediolateral oblique or craniocaudal mammographic image, was 18 mm (range, 4–53 mm). The lesion size was 4–10 mm for 28 lesions, 11–20 mm for 23 lesions, 21–30 mm for 14 lesions, and 31–53 mm for 12 lesions. The morphologies and distributions of calcifications were classified as punctate in 19 lesions, amorphous in 23 lesions, coarse heterogeneous in 9 lesions, pleomorphic in 9 lesions, linear in 5 lesions, and fine-linear branching in 12 lesions; and as clustered in 61 lesions, segmental in 9 lesions, and regional in 7 lesions, respectively. The final assessment of the 77 breast microcalcifications prior to biopsy was category 4a (low suspicion) for 48 (62%) lesions, category 4b (intermediate suspicion) for 24 (31%) lesions, category 4c (moderate suspicion) for 3 (4%) lesions, and category 5 (highly suggestive of malignancy) for 2 (3%) lesions.

Characterization of all lesions seen at US elastography was confirmed by either US-guided vacuum-assisted biopsy alone ($n=37$) or subsequent surgical excisions ($n=40$) which were performed for all lesions with malignant findings, three lesions with atypical ductal hyperplasia, and four lesions with benign findings at needle biopsy histology due to the request of a clinician or a patient. Three atypical ductal hyperplasia lesions at needle biopsy were proven to be low grade DCIS in two lesions and benign ductal epithelial hyperplasia in one lesion on subsequent surgical excision, respectively. In the end, of the 77 lesions, 42 (55%) were benign and 35 (45%) were malignant. Benign lesions were then divided into proliferative and nonproliferative lesions. Proliferative lesions ($n=15$) included six epithelial hyperplasias, five sclerosing adenoses, and four fibroadenomas. Nonproliferative lesions ($n=27$) included 25 fibrocystic changes and two duct ectasias. Malignant lesions included 25 DCIS and 10 IDC with DCIS. Of the ten IDC with DCIS, the initial biopsy histology was DCIS alone in seven cases which were later demonstrated to have IDC components based on surgical histology. Of the 25 DCIS, six lesions were low grade and 19 lesions were high grade. The histological diameters of the lesions, which had been measured at surgical histology without inclusion of the tissue excised by vacuum-assisted biopsy, were 1–70 mm (mean, 23.3 mm) for DCIS and 7–48 mm (mean, 25.7 mm) for IDC with DCIS. The histological diameters of the IDC components alone were 1–10 mm (mean, 6.4 mm). All of the patients with benign lesions underwent follow-up for at least 12 months (mean, 15.9 months; range, 12–23 months) and lesion stability was confirmed.

US data acquisition

A radiologist with 6 years' experience in the interpretation of mammography and breast US obtained US strain images for microcalcifications by using an EUB-8500 scanner (Hitachi Medical, Tokyo, Japan) with a 14–6 MHz linear transducer. US lesions associated with microcalcifications that corresponded to mammographic lesions were first searched with B-mode imaging. The lesion size, shape, depth, and subcutaneous fat arrangement around calcifications seen on mammography were carefully correlated with the findings seen on US. Subsequently, US elastography was performed for the most prominent hypoechoic lesion around the hyperechoic foci. A region of interest (ROI) box was set to include the area from the subcutaneous fat layer to the superficial portion of the pectoralis muscle layer and to focus on the target lesion. The target lesion was vertically compressed by the transducer with light pressure. The elasticity image was displayed by 256 color mapping for each pixel according to the degree of strain within the ROI, using a scale from red (greatest strain; softest component), green (average strain; intermediate component) to blue (no strain; hardest component). The pressure and speed of compression were adjusted to depict the subcutaneous fat layer as mixed red and green and the muscle layer as blue. Real-time monitoring of images and feedback on manual compression were performed to avoid interruption of color encoding during data acquisition using a split screen display showing both B-mode and strain images. The data acquisition procedure took approximately 2–3 min per case. Real-time imaging files were saved as cine clips of at least 10 s (270 frames) per case in the avi format on a hard drive for later review.

US-guided vacuum-assisted biopsy

Immediately after elastographic data acquisition, a histological diagnosis was obtained for all women through US-guided 11-gauge vacuum-assisted biopsy (Mammotome; Ethicon Endo-surgery, Cincinnati, OH). All biopsy specimens underwent specimen radiography (at 22 kVp, 8 mAs, $\times 1.8$ magnification) using a digital mammography unit (Senographe 2000D FFDM; GE Medical Systems, Milwaukee, WI) to confirm calcification retrieval. After the biopsy, a localizing clip (MicroMark II; Ethicon Endo-surgery, Cincinnati, OH) was deployed and post-biopsy mammography was performed to confirm accurate acquisition of elastographic images and sampling of biopsy specimens for the target lesion.

Image evaluation

Two dedicated breast radiologists who had not performed the US examinations analyzed the randomly ordered cine

clips including B-mode and strain images by the split screen method. The radiologists classified the elasticity score in consensus without information of the histological or mammographic findings. B-mode US findings were evaluated with masking of the elastographic images. The examining radiologists had 5 and 11 years of experience in the interpretation of mammography and performing US examinations. The elasticity score was classified from 1 to 3, based on the degree of strain in the hypoechoic lesion.

Table 1 Patient age, mammographic findings, US findings, and final assessment categories of the 77 lesions with suspicious lesions with microcalcifications

Features	Benign lesions (n=42)	Malignant lesions (n=35)
Mean patient age \pm SD (years)	43.4 \pm 9.0	48.2 \pm 8.1
Breast composition		
Density 1	0 (0)	3 (100)
Density 2	5 (39)	8 (62)
Density 3	26 (57)	20 (44)
Density 4	11 (73)	4 (27)
Lesion size (mm)		
4–10	13 (46)	15 (54)
11–20	12 (52)	11 (48)
21–30	8 (57)	6 (43)
31–53	9 (75)	3 (25)
Calcification morphology		
Punctate	15 (79)	4 (21)
Amorphous	12 (52)	11 (48)
Coarse heterogeneous	7 (78)	2 (22)
Pleomorphic	4 (44)	5 (56)
Linear	3 (60)	2 (40)
Fine-linear branching	1 (8)	11 (92)
Calcification distribution		
Clustered	32 (53)	29 (48)
Segmental	3 (33)	6 (67)
Regional	7 (100)	0 (0)
US finding		
Ductal irregularity with echogenic foci	26 (57)	20 (43)
Mass with echogenic foci	16 (52)	15 (48)
Final assessment category		
4a	37 (77)	11 (23)
4b	5 (21)	19 (79)
4c	0 (0)	3 (100)
5	0 (0)	2 (100)

Data are numbers of lesions, numbers in parentheses are rounded percentages

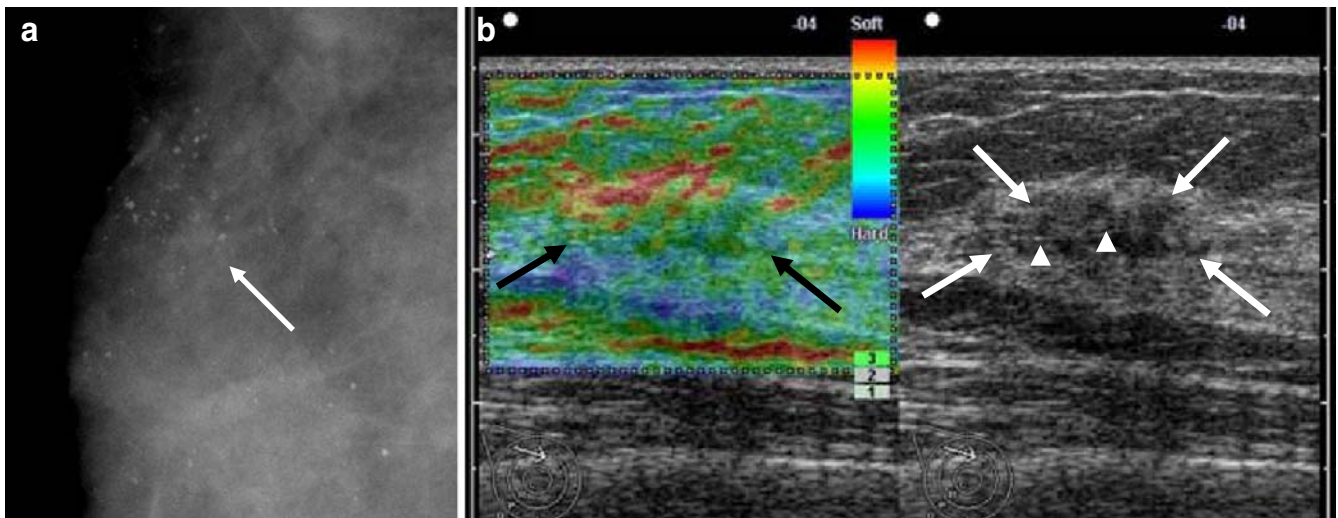


Fig. 1 Images obtained in a 34-year-old woman with microcalcifications detected by screening mammography in the right breast. **a** Magnified mediolateral oblique mammogram demonstrates a 16-mm-diameter cluster of pleomorphic microcalcifications (*arrow*). The final assessment was BI-RADS category 4b. **b** US strain and B-mode images on split screen mode. *Right* B-mode image shows an ill-defined, hypoechoic lesion (*white arrows*) with internal echogenic dots (*arrowheads*) corresponding to the microcalcifications.

Left With elastography, the entire lesion appears shaded in *green* (*black arrows*) with focal *red spots*, indicating greatest to average strain and an elasticity score of 1 (high strain). The subcutaneous fat shows a mixed *red* and *green* color. The *color bar* indicates the degree of strain within the ROI box and the *number bar* indicates the speed of compression. Histologic analysis yielded a diagnosis of fibrocystic change

When the entire lesion was depicted as red to green (greatest to average strain) without blue (no strain) area, it was classified as score 1. When a lesion had both green (average strain) and blue (no strain) areas, it was classified as score 2. A score 3 was assigned when a lesion had a blue (no strain) area over the entire lesion.

Data analysis

Patient age, mammographic features (breast composition, lesion size, shape, and distribution), and the final assessment category were compared between benign and malignant lesions as determined by the histology. B-mode

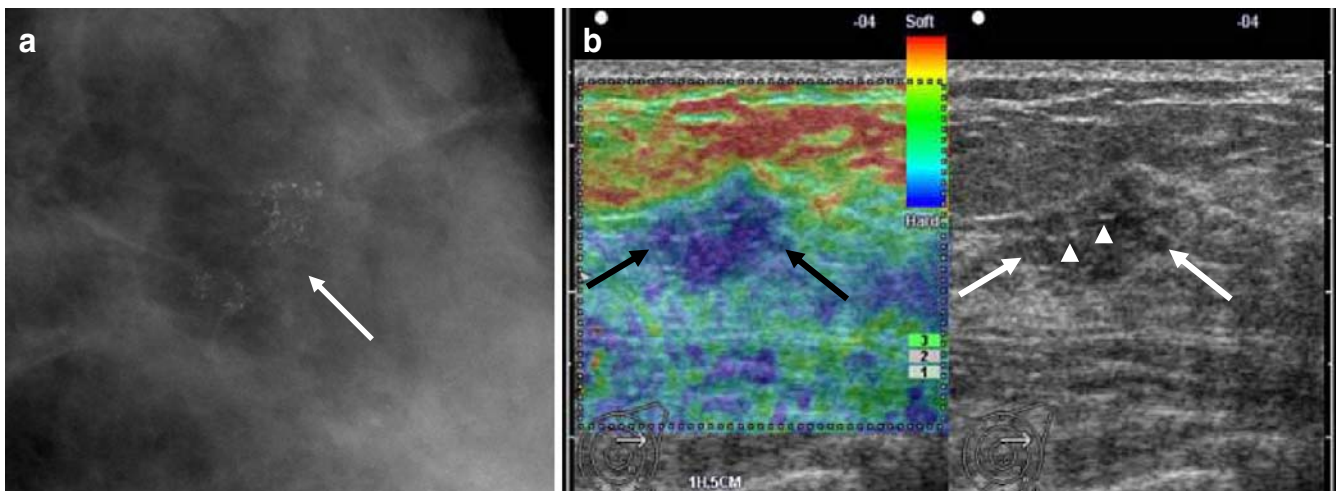


Fig. 2 Images obtained in a 48-year-old woman with microcalcifications detected by screening mammography in the left breast. **a** Magnified craniocaudal mammogram demonstrates an 11-mm-diameter cluster of pleomorphic microcalcifications (*arrow*). The final assessment was BI-RADS category 4b. **b** US strain and B-mode image on split screen mode. *Right* B-mode image shows an ill-defined, hypoechoic lesion (*white arrows*) with internal echo-

genic dots (*arrowheads*) corresponding to the microcalcifications. *Left* With elastography, the entire lesion is *blue* (*black arrows*), indicating no strain and an elasticity score of 3. The subcutaneous fat shows a mixed *red* and *green* color. The *color bar* indicates the degree of strain within the ROI box and the *number bar* indicates the speed of compression. Histologic analysis yielded a diagnosis of high grade ductal carcinoma in situ

Table 2 Histological outcome of the 77 lesions according to the elasticity score

Elasticity score ^a	Benign (<i>n</i> =42)		Malignancy (<i>n</i> =35)		
	Nonproliferative disease (<i>n</i> =27)	Proliferative disease (<i>n</i> =15)	DCIS, low grade (<i>n</i> =6)	DCIS, high grade (<i>n</i> =19)	IDC (<i>n</i> =10)
1	17 (63)	9 (33)	0	1 (4) ^b	0
2	7 (28)	5 (20)	2 (4)	9 (36)	3 (12)
3	3 (13) ^c	1 (4) ^d	4 (13)	9 (39)	7 (30)

Data are the numbers of lesions, numbers in parentheses are rounded percentages

^aA score was assigned according to the degree of strain in the hypochoic lesion. When the entire lesion was red to green without a blue area, the score was 1. When the entire lesion was blue, the score was 3. When the lesion had both green and blue areas, the score was 2

^bSurgical histology revealed a 0.7-cm-sized high grade DCIS

^cBiopsy histology revealed fibrocystic changes

^dBiopsy histology revealed a 0.7-cm sized fibroadenoma

US findings were compared between the two groups by using Fisher's exact test.

To evaluate the difference in strain between US lesions associated with benign and malignant microcalcifications, the elasticity score was compared according to the histological diagnosis using the Student's *t* test. To evaluate the performance of elastography for the differentiation of benign and malignant histology, rate of malignancy according to the elasticity score, the sensitivity, specificity, positive predictive value (PPV), negative predictive value (NPV), and the area under the receiver operating characteristic (ROC) curve (*Az*) were calculated. Statistical analyses were performed using the Statistical Package for the Social Sciences (SPSS version 12.0 for Windows, Chicago, IL). *P* values of less than 0.05 were considered to indicate significant differences.

To identify if there was a subgroup of lesions that had suspicious mammographic findings but were able to be followed-up with a more than 98% of NPV based on US elastography, the malignancy rates according to the elasticity score were analyzed with respect to the lesion size and final assessment category.

Results

Patient age, mammographic findings, B-mode US findings, and the final assessment category between benign and malignant calcifications are compared in Table 1. Women with benign calcifications were younger than those with malignant calcifications (mean age, 43.4 versus 48.2 years; *P*=0.018). However, no difference was found in the mean lesion size (19.9±13.7 versus 15.8±9.2 mm; *P*=0.122) and B-mode US findings (*P*=0.816) between benign and malignant calcifications.

In terms of strain difference according to the histology, the mean elasticity score of benign calcifications was lower than that of malignant calcifications (1.5±0.7 versus 2.7±0.7; *P*<0.001) (Figs. 1 and 2). No difference was found in the mean elasticity score between benign nonproliferative (1.5±0.8) and proliferative lesions (1.5±0.6) (*P*=0.831), DCIS (2.6±0.8) and invasive cancers (2.8±0.6) (*P*=0.469) and low grade DCIS (2.7±0.5) and high grade DCIS (2.6±0.8) (*P*=0.812) (Table 2). All invasive cancers (*n*=10) and 96% (24 of 25) of DCIS lesions showed elasticity scores of 2 or 3.

Table 3 Malignancy rate of the elasticity score with respect to lesion size

Lesion size (mm) ^a	Elasticity score			Total
	1	2	3	
4–10 (<i>n</i> =28)	1/7 (14)	5/11 (45)	9/10 (90)	15/28 (54)
11–20 (<i>n</i> =23)	0/7 (0)	4/8 (50)	7/8 (88)	11/23 (48)
21–30 (<i>n</i> =14)	0/6 (0)	3/4 (75)	3/4 (75)	6/14 (43)
31–53 (<i>n</i> =12)	0/7 (0)	2/3 (67)	1/2 (50)	3/12 (25)

Data are the numbers of lesions, numbers in parentheses are rounded percentages

^aLesion size was defined as the greatest diameter on either a mediolateral oblique or craniocaudal mammographic image

Table 4 Malignancy rate of the elasticity score with respect to the final assessment category

Final assessment category ^a	Elasticity score			Total
	1	2	3	
4a (<i>n</i> =48)	1/24 (4)	6/16 (38)	4/8 (50)	11/48 (23)
4b (<i>n</i> =24)	0/3 (0)	6/8 (75)	13/13 (100)	19/24 (79)
4c (<i>n</i> =3)	0	2/2 (100)	1/1 (100)	3/3 (100)
5 (<i>n</i> =2)	0	0	2/2 (100)	2/2 (100)

Data are the numbers of lesions, numbers in parentheses are rounded percentages

^aThe final assessment category was based on mammographic findings

The rate of malignancy according to the elasticity score was 4% (1 of 27) for score of 1, 54% (14 of 26) for score of 2, and 83% (20 of 24) for score of 3. When a cutoff point of the elasticity score between 1 and 2 was used, the US elastography showed a sensitivity of 97% (34 of 35), specificity of 62% (26 of 42), PPV of 68% (34 of 50), and NPV of 96% (26 of 27). Of the lesions with an elasticity score of 1, there was only one case of a malignancy, which was a 0.7-cm-sized DCIS. The area under the ROC curve (Az value) of the elasticity score was 0.852 (95% confidence interval, 0.753–0.923).

With respect to the lesion size, the highest sensitivity and NPV were achieved for lesions larger than 1 cm in diameter (*n*=49); a sensitivity of 100% (20 of 20), specificity of 69% (20 of 29), PPV of 69% (20 of 29), and NPV of 100% (20 of 20). For lesions less than 1 cm in diameter (*n*=28), the US elastography showed a sensitivity of 93% (14 of 15), specificity of 46% (6 of 13), PPV of 67% (14 of 21), and NPV of 86% (6 of 7) (Table 3).

With respect to the final assessment category, for low suspicious (category 4a) lesions (*n*=48), the US elastography showed a sensitivity of 91% (10 of 11), specificity of 62% (23 of 37), PPV of 42% (10 of 24), and NPV of 96% (23 of 24). For intermediate (category 4b), moderate suspicious lesions (category 4c), or highly suggestive of malignant lesions (*n*=29), the US elastography showed a sensitivity of 100% (24 of 24), specificity of 60% (3 of 5), PPV of 92% (24 of 26), and NPV of 100% (3 of 3) (Table 4).

Discussion

In this study, lesions associated with benign microcalcifications (*n*=42) showed a significantly lower elasticity score (softer) than lesions associated with malignant microcalcifications (*n*=35) (1.5 ± 0.7 versus 2.7 ± 0.7 ; $P < 0.001$). For the microcalcifications larger than 1 cm in diameter, 41% (20 of 49) showed strain over the entire hypoechoic lesion (score 1) on US elastography and all of these lesions were found to be benign. In contrast, all cancers, except for a 0.7-cm-sized DCIS lesion, showed no strain areas within the lesion (score 2 or 3) on US elastography.

Our findings are in concordance with in vitro and clinical studies where US elastography was able to differentiate benign and malignant breast lesions and where the use of US elastography avoided the need for a biopsy in some cases [12–19]. The focus of our study, however, was elastographic evaluation of suspicious microcalcifications, which were seen as ill-defined or microlobulated, hypoechoic masses, or ductal irregularities on B-mode US for both benign and malignant lesions without significant difference ($P=0.816$). As we included lesions with calcifications alone without an obvious mass on mammographic images, 71% (25 of 35) of the malignant lesions were DCIS and the remaining 29% (10 of 35) were IDC that mainly consisted of DCIS components. In our study, a direct elastographic–histologic correlation was made possible through US-guided biopsy of microcalcifications.

An initial in vitro study of breast tissue specimens has demonstrated that DCIS have more complex elastic modulus than other breast tissues. DCIS was softer than normal glandular and fibrous tissues at low strain levels, but much stiffer than normal glandular and fibrous tissues at high strain levels. The elastic moduli of DCIS were less than those of IDC (five times greater than normal glandular tissues for DCIS versus eight times for IDC) even at high strain levels [11]. We used a three-point scale scoring system instead of a five-point scale system used in previous clinical studies [14, 19] because lesions with microcalcifications tend to show less strain difference from surrounding parenchyma contrary to solid mass lesions. So, a smaller scale scoring system was thought to be adequate for the evaluation of microcalcifications. In addition, a larger scale system might have increased interobserver variability. Previous studies, including six and nine cases of DCIS, respectively, showed that the elasticity score of DCIS was between those of benign and invasive cancers [14, 19]. Our study, however, showed that invasive cancers had a similar mean elasticity score (2.8 ± 0.6) as DCIS (2.6 ± 0.8) ($P=0.469$), which was probably due to the relatively small size of IDC cases in our study and the different criteria of the elasticity scoring system.

Our results showed a relatively high sensitivity (97%, 34 of 35), NPV (96%, 26 of 27), and Az value (0.852) of US elastography for the differentiation of benign and malignant

microcalcifications. In the subgroup analysis, 100% sensitivity and NPV were achieved for lesions larger than 1 cm in diameter and for intermediate (category 4b), moderate suspicious (category 4c), or highly suggestive of malignant (category 5) calcifications. In our study, real-time image evaluation using a cine clip enabled continuous monitoring of the strain contrast changes during compression, which could have increased the sensitivity for the evaluation of subtle strain differences. One false negative case at US elastography was found in our study, which was a 0.7-cm-sized DCIS. In recent studies [14, 19, 21], 0 (0 of 111) to 3% (5 of 146) of cancers were found among lesions showing strain over the hypoechoic lesion (elasticity score of 1) determined using the same equipment used in our study. Histologically, DCIS, mucinous carcinoma, and IDCs less than 1 cm in diameter were found as common causes of false negative interpretations with the use of US elastography. Since these tumors have less of a fibrosis component compared with typical spiculated cancers, it is crucial that compression must be carefully performed to depict small strain differences.

This study has some limitations. First, we only included calcified lesions visible on B-mode US. Thus, we cannot generalize our results for the evaluation of all ranges of suspicious microcalcifications at screening mammography. The sample size was also insufficient to reach a solid conclusion. Second, microcalcifications usually had an ill-defined margin or a discontinuous distribution, and the whole extent of the lesion might not be evaluated by

elastography. We only acquired elastographic data focused on the most prominent area on B-mode US. Also, if some lesions were not biopsied on the basis of this study, there would not be evidence other than what was examined by US elastography. Third, interobserver variability was not assessed in our study. Significant observer variability was observed in reader studies using strain images for the classification of breast masses [15, 16]. Last, we performed the study using only one type of commercially available equipment, and the results might have varied according to the type of equipment and algorithm used for elastography.

In conclusion, benign lesions associated with microcalcifications show more strain than malignant lesions associated with microcalcifications at real-time US elastography. All invasive cancers and 96% of DCIS showed no strain area within the hypoechoic lesion at US elastography. Notably, for lesions larger than 1 cm in diameter, the NPV for an elasticity score of 1 was 100% (20 of 20). Therefore, when a lesion associated with low suspicious microcalcifications larger than 1 cm in diameter is visible on B-mode US and shows strain over the entire hypoechoic lesion on US elastography, the need for a biopsy may be averted. Significant observer variability should be considered for the application of B-mode and strain US for the evaluation of breast microcalcifications.

Acknowledgments This study was supported by a grant (A062260) from the Innovative Research Institute for Cell Therapy, Republic of Korea.

References

1. Stomper PC, Connolly JL, Meyer JE, Harris JR (1989) Clinically occult ductal carcinoma in situ detected with mammography: analysis of 100 cases with radiologic-pathologic correlation. *Radiology* 172:235–241
2. Monsees BS (1995) Evaluation of breast microcalcifications. *Radiol Clin North Am* 33:1109–1121
3. Egan RL, McSweeney MB, Sewell CW (1980) Intramammary calcifications without an associated mass in benign and malignant diseases. *Radiology* 137:1–7
4. Kettritz U, Morack G, Decker T (2005) Stereotactic vacuum-assisted breast biopsies in 500 women with microcalcifications: radiological and pathological correlations. *Eur J Radiol* 55:270–276
5. Jackman RJ, Rodriguez-Soto J (2006) Breast microcalcifications: retrieval failure at prone stereotactic core and vacuum breast biopsy—frequency, causes, and outcome. *Radiology* 239:61–70
6. Burnside ES, Ochsner JE, Fowler KJ et al (2007) Use of microcalcification descriptors in BI-RADS 4th edition to stratify risk of malignancy. *Radiology* 242:388–395
7. Moon WK, Im JG, Koh YH, Noh DY, Park IA (2000) US of mammographically detected clustered microcalcifications. *Radiology* 217:849–854
8. Soo MS, Baker JA, Rosen EL (2003) Sonographic detection and sonographically guided biopsy of breast microcalcifications. *AJR Am J Roentgenol* 180:941–948
9. Soo MS, Baker JA, Rosen EL, Vo TT (2002) Sonographically guided biopsy of suspicious microcalcifications of the breast: a pilot study. *AJR Am J Roentgenol* 178:1007–1015
10. Ophir J, Cespedes I, Ponnekanti H, Yazdi Y, Li X (1991) Elastography: a quantitative method for imaging the elasticity of biological tissues. *Ultrason Imaging* 13:111–134
11. Krouskop TA, Wheeler TM, Kallel F, Garra BS, Hall T (1998) Elastic moduli of breast and prostate tissues under compression. *Ultrason Imaging* 20:260–274
12. Garra BS, Cespedes EI, Ophir J et al (1997) Elastography of breast lesions: initial clinical results. *Radiology* 202:79–86
13. Hall TJ, Zhu Y, Spalding CS (2003) In vivo real-time freehand palpation imaging. *Ultrasound Med Biol* 29:427–435
14. Itoh A, Ueno E, Tohno E et al (2006) Breast disease: clinical application of US elastography for diagnosis. *Radiology* 239:341–350

-
15. Regner DM, Hesley GK, Hangiandreou NJ et al (2006) Breast lesions: evaluation with US strain imaging—clinical experience of multiple observers. *Radiology* 238:425–437
 16. Burnside ES, Hall TJ, Sommer AM et al (2007) Differentiating benign from malignant solid breast masses with US strain imaging. *Radiology* 245:401–410
 17. Scaperrotta G, Ferranti C, Costa C et al (2008) Role of sonoelastography in non-palpable breast lesions. *Eur Radiol* 18:2381–2389
 18. Booi RC, Carson PL, O'Donnell M, Roubidoux MA, Hall AL, Rubin JM (2008) Characterization of cysts using differential correlation coefficient values from two dimensional breast elastography: preliminary study. *Ultrasound Med Biol* 34:12–21
 19. Tan SM, Teh HS, Mancer JF, Poh WT (2008) Improving B mode ultrasound evaluation of breast lesions with real-time ultrasound elastography—a clinical approach. *Breast* 17:252–257
 20. American College of Radiology (2003) Breast imaging reporting and data system—mammography (BI-RADS™), 4th edn. American College of Radiology, Reston
 21. Tohno E, Ueno E (2008) Current improvements in breast ultrasound, with a special focus on elastography. *Breast Cancer* 15:200–204